Revision

# Molecular Modeling of Polymer Composite-Solvent Interactions in Electronic Nose Sensors

Abhijit Shevade, Margaret Amy Ryan*, Margie L. Homer, Allison Manfreda, Hanying Zhou, and Kenneth Manatt

Jet Propulsion Laboratory, California Institute of Technology
4800 Oak Grove Drive, Pasadena CA 91109
USA

We report a molecular modeling study to investigate the polymer-carbon black (CB) composite-analyte interactions in resistive sensors. These sensors comprise the JPL Electronic Nose (ENose) sensing array developed for monitoring breathing air in human habitats. The polymer in the composite is modeled based on its stereisomerism and sequence isomerism, while the CB is modeled as uncharged naphthalene rings (with no hydrogens). The Dreiding 2.21 force field is used for the polymer and solvent molecules and graphite parameters are assigned to the carbon black atoms. A combination of molecular mechanics (MM) and molecular dynamics (NPT-MD and NVT-MD) techniques are used to obtain the equilibrium composite structure by inserting naphthalene rings in the polymer matrix. Polymers considered for this work include poly(4-vinylphenol), polyethylene oxide, and ethyl cellulose. Analytes studied are representative of both inorganic (ammonia) and organic (methanol, toluene, hydrazine) compounds. The results are analyzed for the composite microstructure by calculating the radial distribution profiles as well as for the sensor response by predicting the interaction energies of the analytes with the composites.

**Keywords:** Electronic nose, Polymer composite, Molecular modeling, Interactions

*Author to whom correspondence should be addressed.

E-mail: mryan@mail1.jpl.nasa.gov, Fax: +818-393-5007

# 1. INTRODUCTION

The ability to monitor the constituents of air in a closed environment is important to NASA for controlling the breathing air quality in human habitats in which air is recycled. At present, air quality on Space Shuttle flights is determined by collecting samples and analyzing them on the ground using laboratory analytical instruments such as a gas chromatography-mass spectrometer (GC-MS). The availability of a miniature, portable instrument capable of identifying contaminants in the breathing environment at parts-per-billion levels would greatly enhance the capability for monitoring the quality of recycled air as well as providing notification of the presence of potentially dangerous substances from spills and leaks. To fill this need, JPL is developing an Electronic Nose (ENose) for air quality monitoring [1-3].

An electronic nose is an array of chemical sensors which respond when exposed to vapors. Each sensor is non-specific to any one vapor. Upon exposure to a vapor, the sensors respond, creating a pattern across the array. The pattern of distributed response may be deconvoluted, and the contaminants identified and quantified using a software analysis program such as pattern recognition and/or neural network or principal component analysis. Electronic noses have been discussed by several authors and may be applied to quality control and environmental monitoring in fields such as food processing, medical and industrial environmental monitoring [2,3-11].

The Electronic Nose (ENose) developed at JPL uses an array of polymer-carbon black composite sensing films [1-3]. The addition of carbon black to an insulating polymer matrix makes the film conducting. The conductivity is the result of the formation of carbon black conductivity networks in the polymer matrix. Upon exposure to organic vapors, the polymer

matrix swells, resulting in the breaking of some of the carbon black conductive networks and hence causing a change in the sensor response [1,11].

The selection of sensors for an array should be based on the list of analytes one wishes to identify. Acquiring experimental data for one set of analytes and optimizing the array for selectivity, sensitivity and stability is time and labor intensive. If new analytes are selected, it would be convenient to a priori be able to know the predicted responses of potential sensors to new analytes; then the array can be optimized with less extensive experimental testing. Hence, an approach based on molecular modeling will not only help in providing a fundamental understanding of the molecular level processes related to polymer composite-solvent interactions but also will set protocols for optimizing the array matrix. Thus, theoretical and computational approaches coupled with experimental efforts will be a key in selecting and developing new improved materials in a more rational way [12].

The underlying objective of this work is to develop molecular models which accurately describe polymer-carbon black (CB) composite films used in the ENose sensors and to gain a detailed understanding of their interactions with target analyte molecules. Polymers considered for this work include poly(4-vinylphenol), polyethylene oxide, and ethyl cellulose. These polymers will be referred to as PVPh, PEO and EC and the carbon black will be referred to as CB in the following discussion. The target analytes studied are representative of both inorganic (ammonia) and organic (methanol, toluene, hydrazine) class of compounds and are molecules that are monitored for on an International Space Station. A combination of molecular simulation tools (molecular mechanics and dynamics) is used to obtain the composite model and also evaluate its interaction with analytes.

Section 2 of this paper describes the models for the polymer, carbon black and also outlines an approach used to develop the final composite model. The simulation details are discussed in section 3. The microstructure details of the composite films and their interactions with the analytes are discussed in section 4.

## 2. MOLECULAR MODELS

The molecular simulations were performed on a Silicon Graphics O2 workstation, using the commercial software Cerius$^2$ [13].

### 2.1 Polymer

The polymer model is based on its stereisomerism (tacticity) and sequence isomerism (connectivity). The polymer tacticity results in three possible arrangements of the side groups (or pendant groups) around the polymer backbone. The side groups could either be on one side (isotatctic) or on alternate sides (syndiotactic) or randomly arranged (atactic) around the polymer backbone. The connectivity of the monomer units could either be head-to-tail or tail-to-tail or head-to-head. The polymer monomer units considered for this work are shown in Figure 1.

### 2.2 Carbon black (CB)

The CB structure typically consists of spheroidal particles fused to each other. Within each of these particles, carbon atoms are arranged in imperfect graphite layers [14]. The CB in the present work is modeled as naphthalene rings (i.e., small graphite sheets) with no hydrogen as it is difficult to insert large graphite sheets in a high-density polymer matrix.

### 2.3 Polymer-carbon black composite

Sensing film for the JPL ENose was made by dissolving the polymer in a solvent or solvent mixture, dispersing the carbon black in the polymer solution, pipetting the composite solution onto the sensor substrate, and allowing the solvent(s) to evaporate [1-3]. The model for the polymer-CB composite film is being developed by adopting a strategy that involves performing simulations first under "no solvent" and then under "solvent" conditions.

#### 2.3.1 No- solvent conditions

The composite model is initially developed under no-solvent conditions (or vacuum). To begin with, the density of the polymer-CB composite film ($\rho$) is approximated as a linear combination of the sum of bulk density of individual components times their weight fractions, i.e., $\rho = \rho_p x_p + \rho_{cb} x_{cb}$ (where, $\rho_p$ = polymer density, $\rho_{cb}$ = carbon black density, $x_p$=weight fraction of the polymer and $x_{cb}$=weight fraction of the carbon black). The densities of the different polymers and CB and used in the current study are listed in Table 1. The JPL ENose films are made with polymer weight fraction of 0.75-0.8 [1-3]. A value of $x_p$ =0.75 was considered for the current composite model development. An amorphous polymer unit cell was built with a density $\rho_p x_p$ containing two polymer chains each containing *m* monomer units. The naphthalene rings were then inserted in the polymer matrix until the composite film density $\rho$ was reached. The entire system is then equilibrated by MM followed by NVT-MD simulations at 300 K.

### 2.3.2 Solvent conditions

The composite structure obtained under "no solvent conditions" is then subjected to solvent conditions. The composite structure obtained from the previous step is immersed in a large solvent box. This step is done to mimic the polymer-carbon black solution, which is used in solvent casting of the sensor films. The entire system (composite+solvent) is then equilibrated by MM followed by NVT-MD simulations at 300 K.

### 2.3.3 Film formation

On reaching equilibrium, the solvent molecules are removed (this step corresponds to deposition of the film and evaporation of the solvent from the sensor film, as done under experimental conditions) and the box is compressed to the target density ρ, followed by density and structural relaxation using NPT-MD and NVT-MD simulations at 300 K, respectively to achieve the final equilibrium structure and density.

## 3. SIMULATION

The total energy of a system is a sum of its kinetic and potential energy. While the system kinetic energy depends on the temperature, the total system potential energy ($U_{total}$) can be written as a superposition of short range valence ($U_{valence}$) and long range non-bonded interactions ($U_{non-bond}$)

$$U_{total} = U_{valence} + U_{non-bond} \,, \tag{1}$$

where the valence (or internal) terms consist of bond stretching ($U_{bond}$), bond-angle bending ($U_{bend}$), dihedral angle torsion ($U_{torsion}$) and inversion ($U_{inversion}$) terms

$$U_{valence} = U_{bond} + U_{bend} + U_{torsion} + \mathrm{U}_{\mathrm{inversion}} \,, \tag{2}$$

For the polymer composite, the valence term contribution to the potential energy comes from the polymer chains and the carbon black molecules. The non-bond interaction term includes polymer-polymer, polymer-carbon black and carbon black-carbon black interactions. The non-bond (or external) interactions consist of van der Waals ($U_{vdw}$) and electrostatic ($U_Q$) terms

$$U_{non-bond} = U_{vdw} + U_Q \,, \tag{3}$$

The $U_{vdw}$ term takes into account the intermolecular interactions and the interactions between atoms that are separated by three or more bonds within a chain.

### 3.1 Building of the amorphous polymer box

The amorphous polymer box is built by first constructing a polymer chain based on its tacticity and connectivity. The atactic nature of poly(4-vinyl phenol) is assumed (i.e., the phenol groups randomly arrange with respect to the carbon backbone). No such assumption is necessary for the polymers PEO and EC, which have no tacticity centers. Head-to-tail connectivity of the monomers

is assumed for all the polymers. The number of monomer units (m) is selected so as to keep the number of atoms in the composite model close to two thousand.

The charges of isolated polymer chains are based on the charge equilibration method (Qeq) [15]. The polymer chains were initially minimized by molecular mechanics and then by molecular dynamics for 10ps (time step = 0.001 ps) at 300 K. This was then followed by running annealing dynamics for 10ps, in which the system temperature is varied in cycles from one temperature to another and back again. In our case, temperatures were varied in increments of 50 K for a cycle from 300 K to 500 K and back. This annealing was done so as to relieve the stresses in the polymer chain. The Dreiding 2.21 force field [16] was used for the polymers.

An amorphous unit cell containing one polymer chain and of density $\rho_p x_p$ was then built using the AMORPHOUS builder module in the software. The unit cell containing one polymer is replicated in the x direction to form a superlattice containing two polymer chains. The amorphous polymer box was then minimized by both MM and NVT-MD at 300 K before the naphthalene rings were inserted.

### 3.2 Polymer-carbon black composite model development

The carbon black, modeled as naphthalene rings (i.e., small graphite sheets) with no hydrogens, are inserted in the polymer matrix by performing a cavity search in the polymer matrix. The carbon atoms of the naphthalene rings have no charge and were assigned graphite parameters [17]. A cavity of radius 3.5-4 °A was used to determine possible locations for the naphthalene rings in the polymer matrix. The cavity could be searched either by using a grid search or by random cavity search [18]. A random cavity search was used for this work. The naphthalene rings are inserted in the amorphous

polymer box until a starting model density $\rho = \rho_p x_p + \rho_{cb} x_{cb}$ (as discussed in the previous section) of the composite is reached. Density and structural relaxation for the polymer-CB composite was then achieved by performing molecular mechanics followed by NVT- molecular dynamics simulation at 300 K. The attainment of equilibrium was judged by monitoring the total energy of the composite. (This is shown in Figure 2, described below). Equilibrium was assumed if the change in system potential energy was less than 5 kcal/mol over 50 ps simulation run.

The next stage in the composite model development involves equilibrating the composite model in the solvent. A unit cell with the desired solvent composition was initially created and minimized by MM. A superlattice of the solvent box was then created so as to have ~ 5000 solvent atoms in the system. The solvent box is then equilibrated by both NPT-MD and NVT-MD to get the right density and equilibrium structure.

The composite structure was then immersed in the solvent box. Solvent molecules that are closer than 1.4 $^{o}$A to the polymer and naphthalene rings were excluded to avoid infinite force problems. The composite structure was then equilibrated by MM to remove close contacts followed by NVT-MD. Upon achieving equilibrium (based on monitoring the total energy of the system), the solvent molecules are excluded and the box is recompressed to the starting density, $\rho$. The structure is then optimized again, finally using both NPT-MD and NVT-MD. The equilibrium was assumed if the change in potential energy of the system was less than 2 kcal/mol over 100 ps simulation run.

# 4. RESULTS AND DISCUSSION

## 4.1 Development of the composite model

Immersing the composite in the solvent box mimics the composite solutions used for film casting. Figures 2(a), (b) and (c) shows the convergence of the potential energy of the composite structure in the solvent by performing NVT-MD simulations at 300 K using a time step of 0.001ps.

The final composite structures of the three polymers are shown in Figures 3(a), (b) and (c). These are obtained after removing the solvent, recompressing the box to the initial density and equilibrating it is using NPT-MD and NVT-MD techniques at 300 K. The pressure for the NPT simulations is set to atmospheric pressure. Figure 4 show the density versus time plots of the composite after performing NPT-MD simulations at 300 K for the final structure. The final predicted densities are ordered, PVPh> EC > PEO. The convergence of the potential energy of these structures by NVT-MD simulations are shown in Figures 5(a) (b) and (c). A comparison of the stability of these structures based on these energies is not possible due to the different solvents recepies used for the film casting. On an average the composite structures take a few nanoseconds of MD simulations to equilibrate. Furthermore, the PEO composite needs more time to equilibrate, compared to the other polymer composites. This could be due to the low glass transition temperature possessed by PEO resulting in more flexibility of the polymer chains.

### 4.2 Analysis of polymer composite microstructure

Polymer composite microstructure could be evaluated by calculating the radial distribution profiles, g(r), from the trajectories of the composite structure. The radial distribution function is the ratio of local density of the atoms to the system density. It gives the number of atoms found at a given distance in all directions seen from an atom of interest [19]. We would like to know how the naphthalene rings arrange with respect to the polymer backbone in the composite. This could provide an insight to the percolation behavior in polymer-CB composites where the addition of the CB imparts conductivity to the film by coating the polymer and also forming networks in the polymer matrix [20]. Figure 6(a) shows the radial distribution function of the naphthalene rings with respect to the carbon atoms of the polymer backbone. The $sp^3$ hybridized carbon atoms on the polymer backbone were used for the radial distribution calculations of the PVPh and PEO polymers, while for EC, the carbon atoms that forms the cellulose backbone (ring carbon atoms) were considered for calculations. It can be seen that the naphthalene rings cluster more around the polymer backbone as compared to the other polymer composites. For the PVPh composite as shown in Figure 6(b), the naphthalene rings tend to cluster around the phenol rings as compared to the polymer backbone.

### 4.3 Interaction of analytes with polymer composite

The Spacecraft Maximum Allowable Concentration (SMAC) is the maximum concentration of an analyte permissible aboard a space station [21]. The SMAC values of the analytes considered for the present study are shown in Table 2. For most compounds, these concentrations are in single to tens of parts-per-million (ppm) range. It is difficult to perform sorption simulation studies at such low partial pressures of the analyte using the software (experiments being performed at

atmospheric pressure) and could lead to no molecules being inserted into the system. Therefore, we considered only one analyte molecule to calculate the interaction energies of the analyte with the composites. The contributions to the total interaction energy of an analyte with the composite as shown in equation (4) is from its interactions with the polymer chains, CB molecules and other analytes. Since we have only one analyte molecule, the analyte-analyte interactions will not contribute to total interaction energy.

$$U_{composite-analyte} = U_{polymer-analyte} + U_{carbonblack-analyte} \quad (4)$$

The simulations were performed using the SORPTION module in the Cerius$^2$ software at a fixed loading of one analyte and at 300 K. The program generates random points in the composite model and tries to insert the analyte molecules. Insertion attempts that involve the overlapping of the analyte molecule with the composite structure are discarded. For each composite-analyte interaction, 2-3 million simulations (analyte insertions) were run and the average energy of composite-analyte interactions was calculated at the end of the simulation. The interaction energies of the polymer composites with ammonia, methanol, toluene and hydrazine are shown in Figures 7(a), (b), (c) and (d), respectively.

It can be seen in Figure 7(a) that for an inorganic molecule such as ammonia, the PEO composites show stronger interaction, as compared to the PVPh and EC composites. The organic molecules also considered for the present study include methanol, toluene and hydrazine. Figure 7(b) shows the interaction of a methanol molecule with the three polymer composites. The order of polymer composite-analyte interaction is PVPh > PEO> EC. This could possibly be due to the strong hydrogen bonds that methanol can form with the first two polymers, PVPh and PEO as

compared to the EC. Hydrazine and toluene molecules show a stronger interaction with the PEO composite, as compared to the PVPh and EC composites. These interactions are shown in Figures 7(c) and (d).

Currently work is in progress for validating the above composite model by comparing it with the experimental findings.

## 5. CONCLUSIONS

A molecular model for the polymer composite was developed by an approach that mimics the experimental composite film casting and formation. The composite model consisted of carbon black modeled as naphthalene rings (with no hydrogens) inserted in an amorphous polymer matrix. The microstructure analysis by using the radial distribution profiles showed the different arrangements of carbon black molecules with respect to the polymer backbone. The sorption studies at fixed analyte loading also predicted different composite-analyte interactions. Composite-analyte interaction energies predict that the PEO-carbon black composite will show strongest sensor response to ammonia, toluene and hydrazine.

## ACKNOWLEDGEMENTS

This research was funded by NASA code UB, Advanced Environmental Monitoring and Control. This work was carried out at the Jet Propulsion Laboratory, California Institute of Technology under the contract with the National Aeronautics and Space Administration.

## REFERENCES


[1] Ryan, M. A, Homer, M. L., Buehler, M. G., Manatt, K. S., Zee, F., and Graf, J., Proceedings of the 27th International Conference on Environmental Systems, Society of Automotive Engineers, Lake Tahoe, Nevada, USA, 1997.

[2] Ryan, M. A., Buehler, M. G., Homer, M. L., Manatt, K. S., Lau, B., Jackson, S., and Zhou, H., The 2nd International Conference on Integrated MicroNanotechnology for Space Applications; Pasadena, CA, USA. 1999.

[3] Ryan, M. A., Homer, M. L., Zhou, H., Manatt, K. S., Ryan, V. S., and Jackson, S. P., Proceedings of the 30th International Conference on Environmental Systems; Toulouse, France, 2000.

[4] Freund, M.S., and Lewis, N. S., Proc. National Academy of Science, 92 (1995) pp. 2652-2656.

[5] Ryan, M. A., and Lewis, N. S., Enantiomer, 6 (2001) pp.159-170.

[6] Thaler, E.R., Kennedy, D.W., and Hanson, C.W., Am J. Rhinol. , 15 (2001) pp. 291-295.

[7] Guernion, N., Ratcliffe, N.M., Spencer-Phillips, P.T.N., and Howe, R.A., Clin. Chem. Lab. Med., 39 (2001) pp.893-906.

[8] Nimmermark, S., Water Sci. Technol., 44 (2001) pp. 33-41.

[9] Magan, N., and Evans, P., J. Stored. Prod. Res., 36 (2000) pp. 319-340.

[10] Di Natale, C., Macagnano, A., Paolesse, R., Tarizzo, E., Mantini, A., and D'Amico, A., Sens. Actuators, B, Chem 65 (2000) pp. 216-219.

[11] Severin, E. J., Doleman, B. J., and Lewis, N. S., Anal. Chem., 72 (2000) pp. 658- 668.

[12] Gubbins, K.E., Chem. Engng. Prog., 85 (1989) pp. 38-49.

[13] Cerius$^2$ v 4.2, Accelrys Inc., San Diego, California, USA.

[14] E. K. Sichel (Eds.), *Carbon Black-Polymer Composites*, Marcel Dekker Inc., New York, 1982.

[15] Rappe, A.K., and Goddard, W.A., J. Phys. Chem., 95 (1991) pp.3358-3363.

[16] Mayo, S.L., Olafson, B.B., and Goddard W.A., J. Phys. Chem., 94 (1990) pp. 8897-8909. .

[17] W.A. Steele, *The Interaction of Gases with Solids Surfaces,* Clarendon Press, Oxford, 1974

[18] Mezei, M., Mol. Phys., 40 (1980) pp. 901-906

[19] Allen, M.P., and Tildesley, D.J. *Computer Simulation of Liquids*, Clarendon Press, Oxford, 1987.

[20] Cheah, K., Simon, G.P., and Forsyth, M., Polym. Int., 50 (2001) pp.27-36.

[21] Spacecraft Maximum Allowable Concentrations for Selected Airborne Contaminants, vols.1 & 2, Academy Press, Washington D.C., 1994.

**Biography**

*Abhijit Shevade* is currently doing his Postdoctoral research at JPL focusing on the modeling of the polymer composite-analyte interactions in Electronic Nose sensors. He obtained his B.S. and M.S. degrees in Chemical Engineering from the University Department of Chemical Technology, University of Bombay, India in 1993 and 1996, respectively. He received his Ph.D. in Chemical Engineering from Kansas State University, USA in 2001. His research interests include molecular modeling of interfacial phenomena.

*Margaret Amy Ryan* is the Principal Investigator of the Electronic Nose project at JPL. She obtained her A.B. degree in History in 1972 from the University of Chicago and a B.S. in Chemistry from the Metropolitan State College of Denver in 1981. She received her Ph.D. in Physical Chemistry from the University of Massachusetts at Amherst in 1987. Her research interests include chemical sensors; including polymer-carbon composite sensor array for space station and shuttle environmental monitoring, all silicon carbide sensors for identification of hydrocarbons and hydrocarbon mixtures and colorimetric sensors. Materials and processes for thermal-to-electric energy conversion- high temperature solid electrolytes; metals as cathodes in high temperature, corrosive environments; electrochemical deposition of semiconductors for thermoelectric applications.

*Margie Homer* is the Co- Investigator of the Electronic Nose project at JPL. She obtained a B.A. in Chemistry from Swarthmore College, Pennsylvania in 1985 and then a Ph.D. in Physical Chemistry from the University of California at Los Angeles in 1993. Her research interest includes chemical sensors.

*Allison Manfreda* is a member of the JPL Electronic Nose team. She works on the experimental aspects of the ENose, including composite film casting and development, and training the sensors for different analytes. She received her B.S. degree in Chemistry from California State Polytechnic University – Pomona in 2002. Her research interests include investigating the effect of physico-chemical properties of analytes and process conditions on the sensors sensitivity and selectivity.

*Hanying Zhou* is a member of the JPL ENose team. She develops data analysis programs to deconvolute the patterns of ENose distributed response. Hanying Zhou received her M. S. in Optical Engineering from Zhejiang University, China in 1988 and a Ph.D. in Electrical Engineering from The Pennsylvania State University in 1995. Between 1988 and 1990, she was a research scientist at Shanghai Institute of Fine Optics and Mechanics, Academia Sinica. Since 1998, she has been with the Jet Propulsion Laboratory where her main research interests include optical pattern recognition and holographic memory.

*Kenneth Manatt* is a member of the JPL ENose team. He helps in designing and programming the Analog and Digital electronics aspect of the ENose sensor device. He received his B.S. in Geology from the University of California Santa Cruz in 1987. He has worked for numerous JPL programs since 1989 as an Analog and Digital electronics designer, programmer.

## Figure captions

**Figure 1:** Monomer structures for (a) poly(4-vinylphenol), (b) polyethylene oxide, and (c) ethyl cellulose polymers.

**Figure 2:** NVT–MD equilibration of solvent-polymer carbon black composite systems for (a) poly(4-vinylphenol), (b) polyethylene oxide, and (c) ethyl cellulose polymers.

**Figure 3:** Final polymer carbon black composite model for (a) poly(4-vinylphenol), (b) polyethylene oxide, and (c) ethyl cellulose polymers. The carbon black clusters are shown in yellow and the polymer chains are shown in cylindrical representation.

**Figure 4:** Density versus time plots of the composite obtained by NPT-MD equilibration after solvent removal from (a) poly(4-vinylphenol), (b) polyethylene oxide, and (c) ethyl cellulose composite systems.

**Figure 5:** NVT–MD equilibration of polymer carbon black composite after solvent removal from (a) poly(4-vinylphenol), (b) polyethylene oxide, and (c) ethyl cellulose composite systems.

**Figure 6:** Radial distribution profiles for the naphthalene rings with the respect to the (a) polymer carbon backbone for all the composites and (b) polymer carbon backbone and phenol oxygen atoms for the poly(4-vinylphenol) composite.

**Figure 7:** Polymer composite–analyte interaction energies for (a) ammonia, (b) methanol, (c) toluene, and (d) hydrazine molecules.

**Table 1: Physical properties of polymer composite components**

| | *Density g/cm$^3$* | | *Glass transition, $^oC$* |
|---|---|---|---|
| | *Polymer* | *Composite$^\$$* | |
| Poly(4-vinylphenol) | 1.163*(1.2) | 1.322 | 150 |
| Polyethylene oxide | 1.127* | 1.295 | -45 |
| Ethyl cellulose | 1.138* (1.14) | 1.297 | 43 |
| Carbon black *(Cabot Black Pearl 2000)* | 1.8 | | |

* Predicted by molecular modeling. The manufacturer's experimental value is shown in the bracket.

$ Starting density for the composite model development.

**Table 2: Spacecraft Maximum Allowable Concentration (SMAC) values for the target analytes** [21]

| *Solvent* | *SMAC (ppm)*<br>*24 hr* |
|---|---|
| Ammonia | 20 |
| Methanol | 10 |
| Toluene | 16 |
| Hydrazine | 0.3 |

**FIGURE 1**

(a)

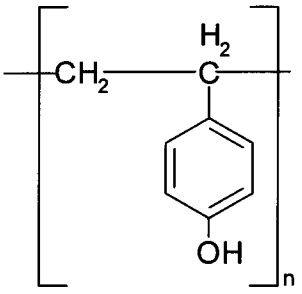
H2
CH2
C
OH
n

(b)

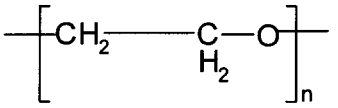
CH2
C
O
H2
n

(c )

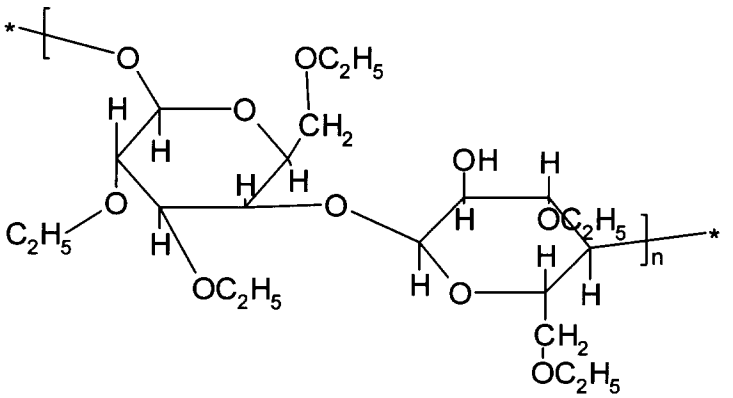
*
O
OC2H5
H
O
CH2
H
H
H
H
OH
H
O
O
H
OC2H5
n
*
C2H5
O
H
H
OC2H5
H
O
H
H
CH2
OC2H5

**FIGURE 2**

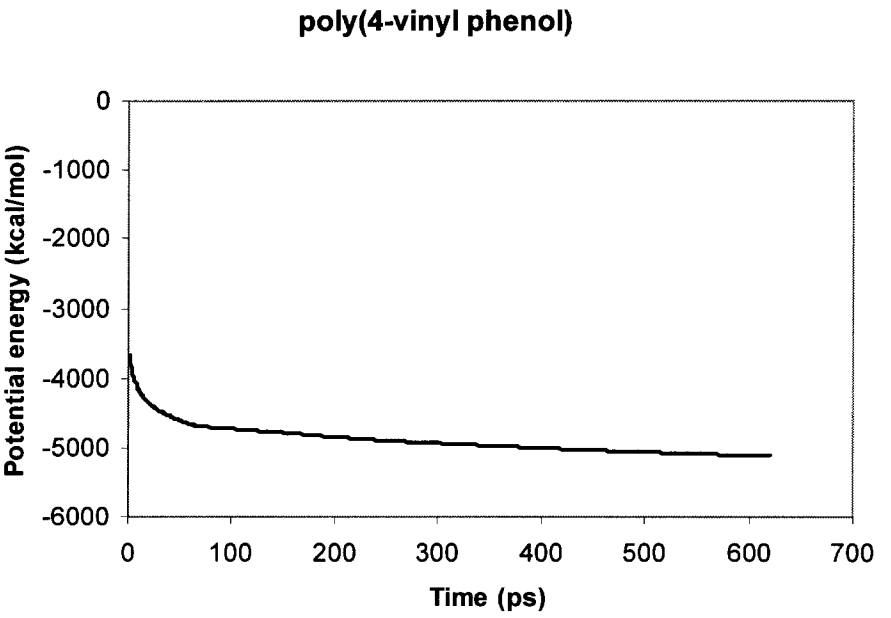
poly(4-vinyl phenol)
Potential energy (kcal/mol)
0
-1000
-2000
-3000
-4000
-5000
-6000
0
100
200
300
400
500
600
700
Time (ps)

(a)

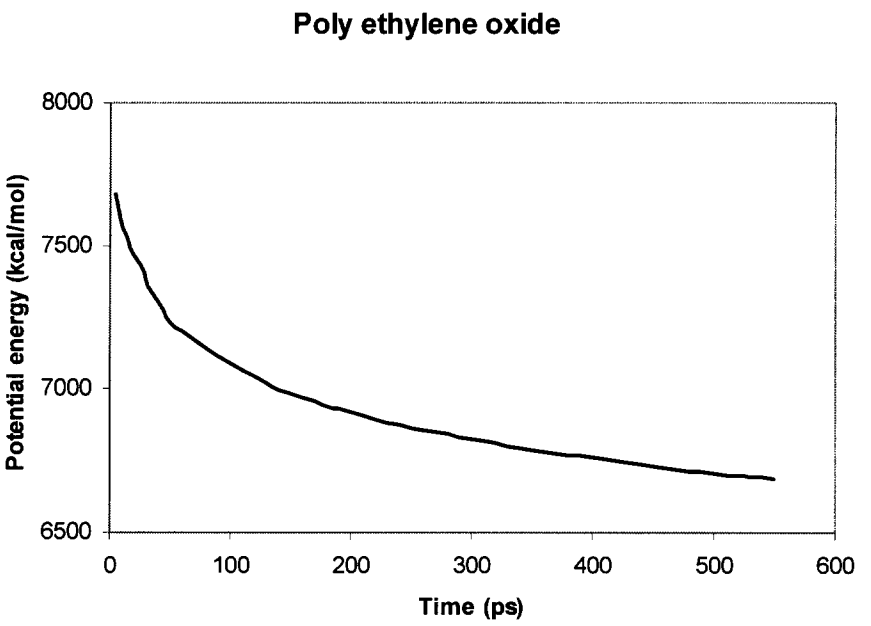
Poly ethylene oxide
Potential energy (kcal/mol)
8000
7500
7000
6500
0
100
200
300
400
500
600
Time (ps)

(b)

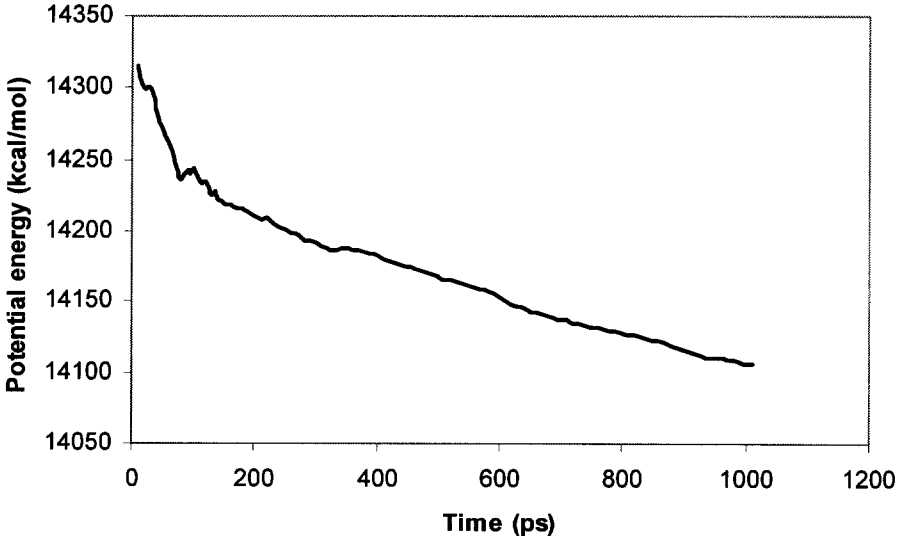
Ethyl cellulose
Potential energy (kcal/mol)
14350
14300
14250
14200
14150
14100
14050
0
200
400
600
800
1000
1200
Time (ps)

(c )

**FIGURE 3**

**Poly(4-vinylphenol)**

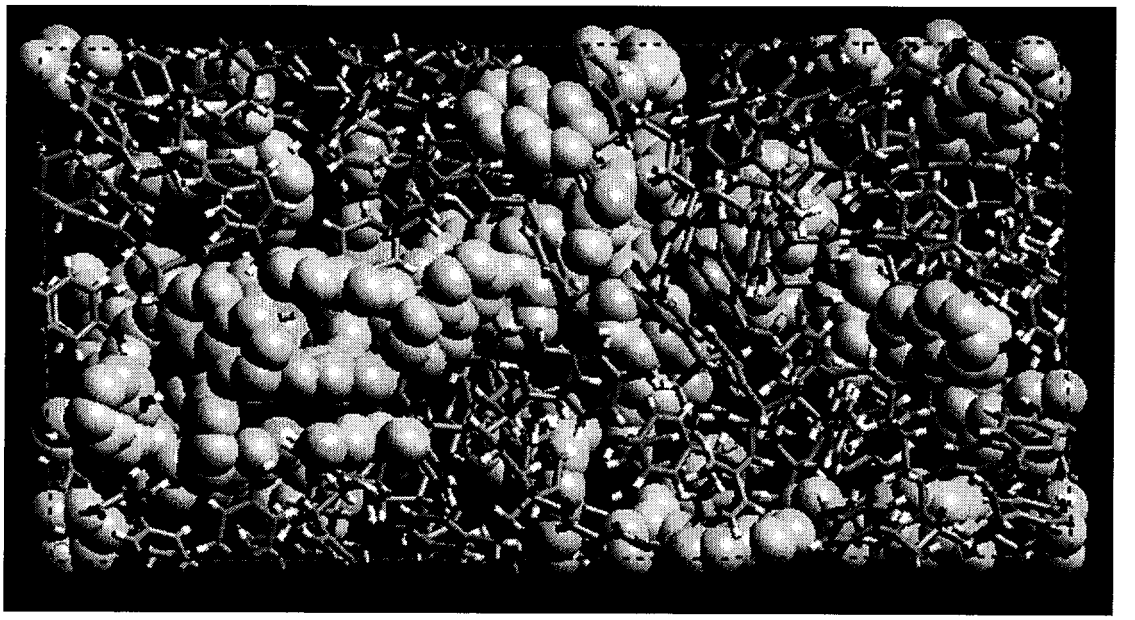

(a)

**Polyethylene oxide**

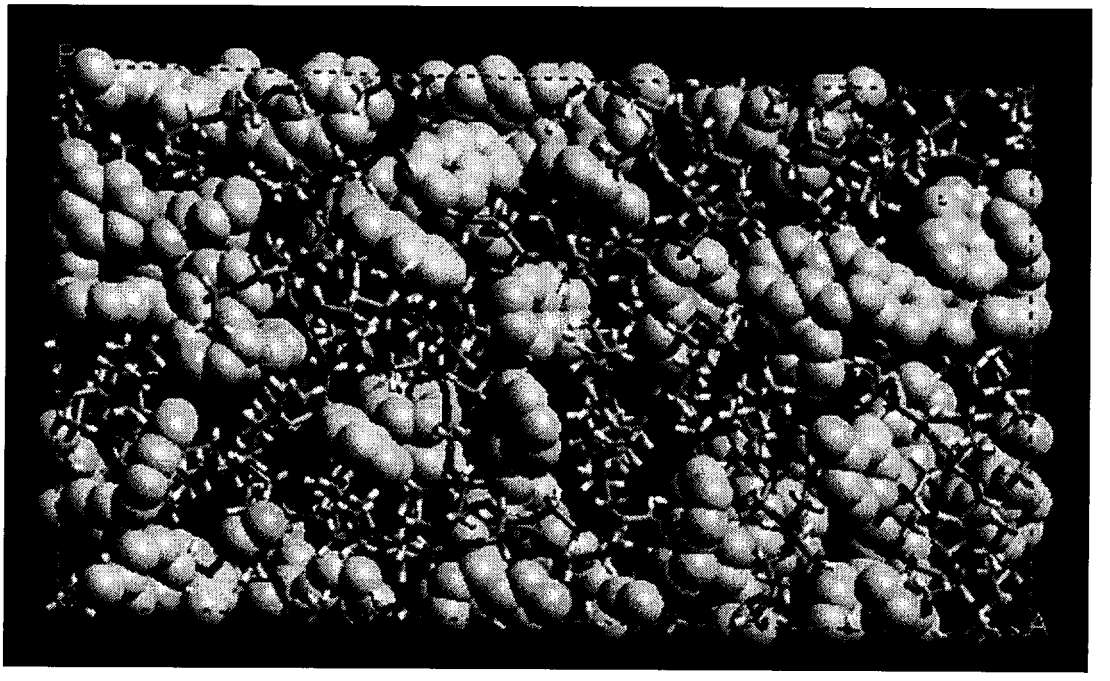

(b)

**FIGURE 3 (Contd.)**

**Ethyl cellulose**

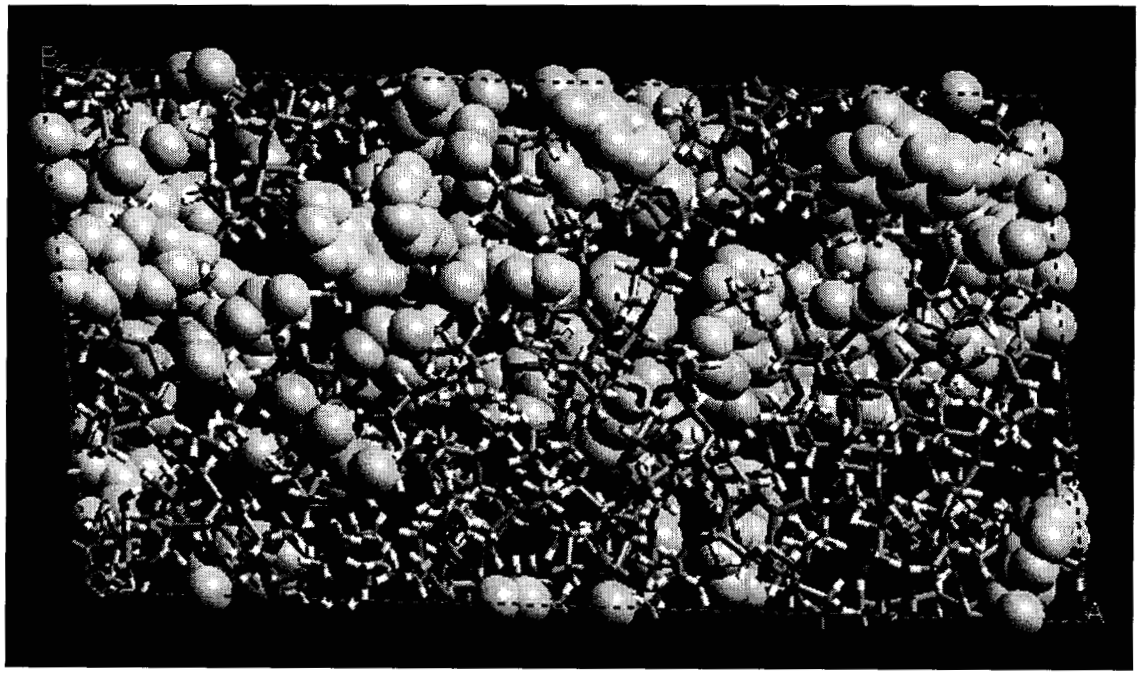

(c)

**FIGURE 4**

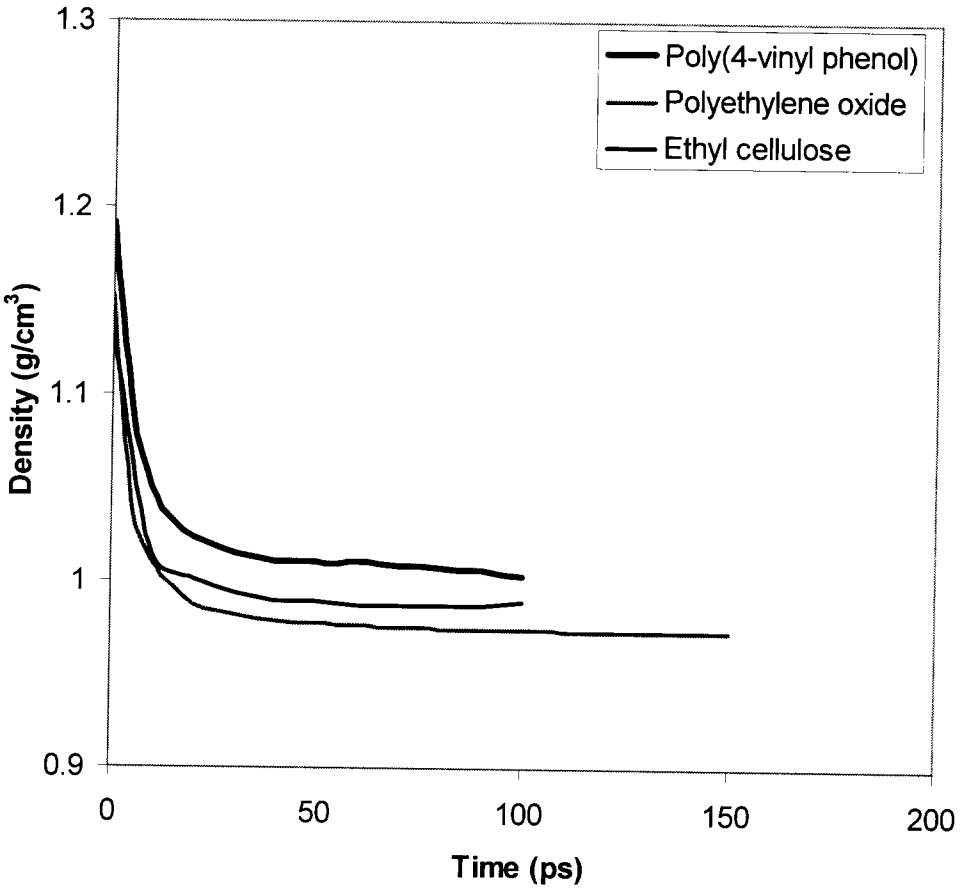
1.3
1.2
1.1
1
0.9
Density (g/cm3)
0
50
100
150
200
Time (ps)
Poly(4-vinyl phenol)
Polyethylene oxide
Ethyl cellulose

FIGURE 5

(a)

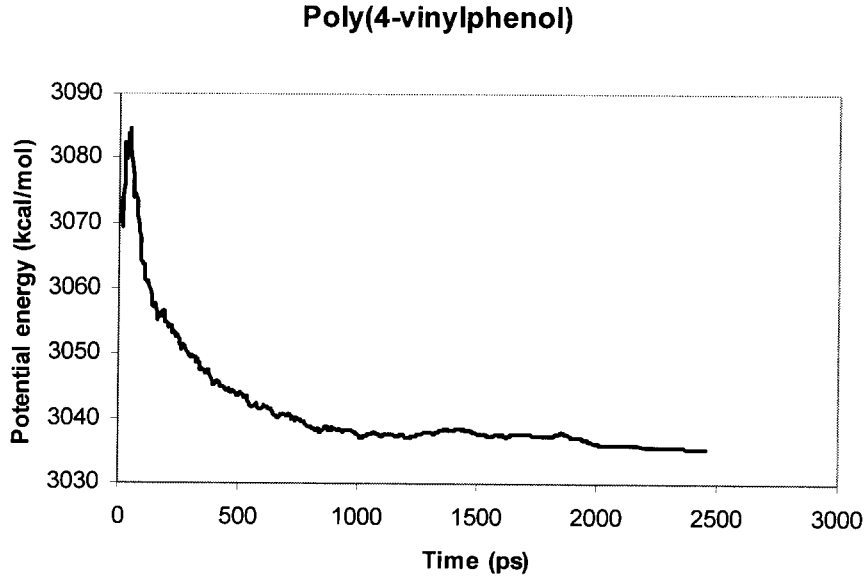
Poly(4-vinylphenol)
Potential energy (kcal/mol)
3090
3080
3070
3060
3050
3040
3030
0
500
1000
1500
2000
2500
3000
Time (ps)

(b)

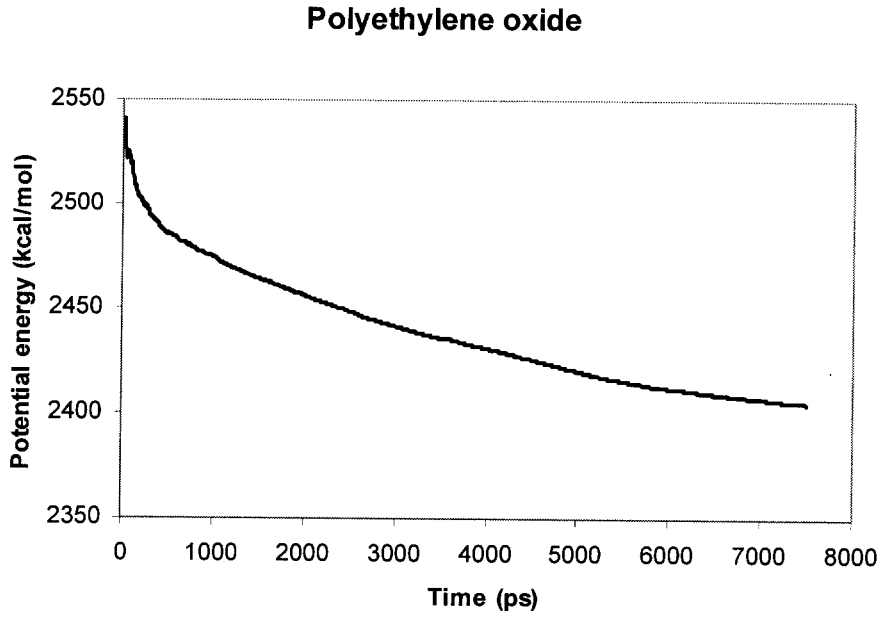
Polyethylene oxide
Potential energy (kcal/mol)
2550
2500
2450
2400
2350
0
1000
2000
3000
4000
5000
6000
7000
8000
Time (ps)

(c )

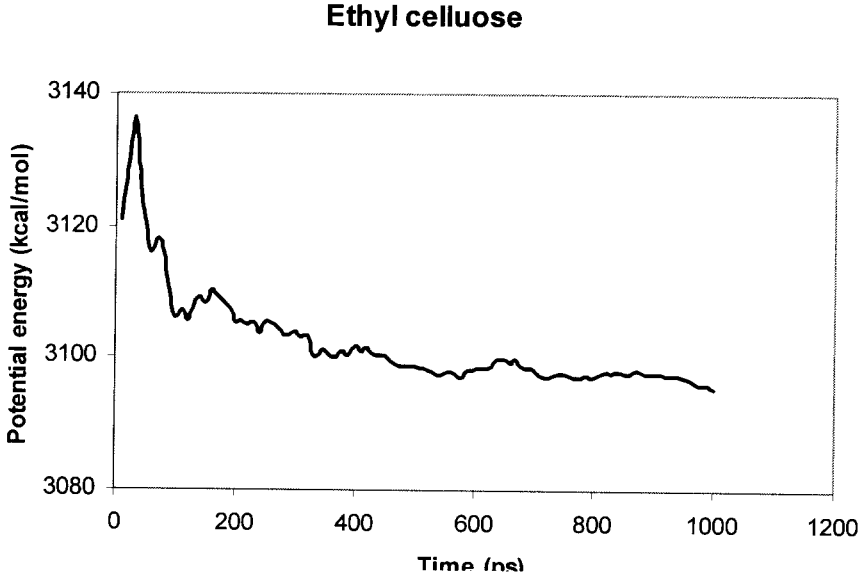
Ethyl celluose
Potential energy (kcal/mol)
3140
3120
3100
3080
0
200
400
600
800
1000
1200
Time (ps)

**FIGURE 6**

(a)

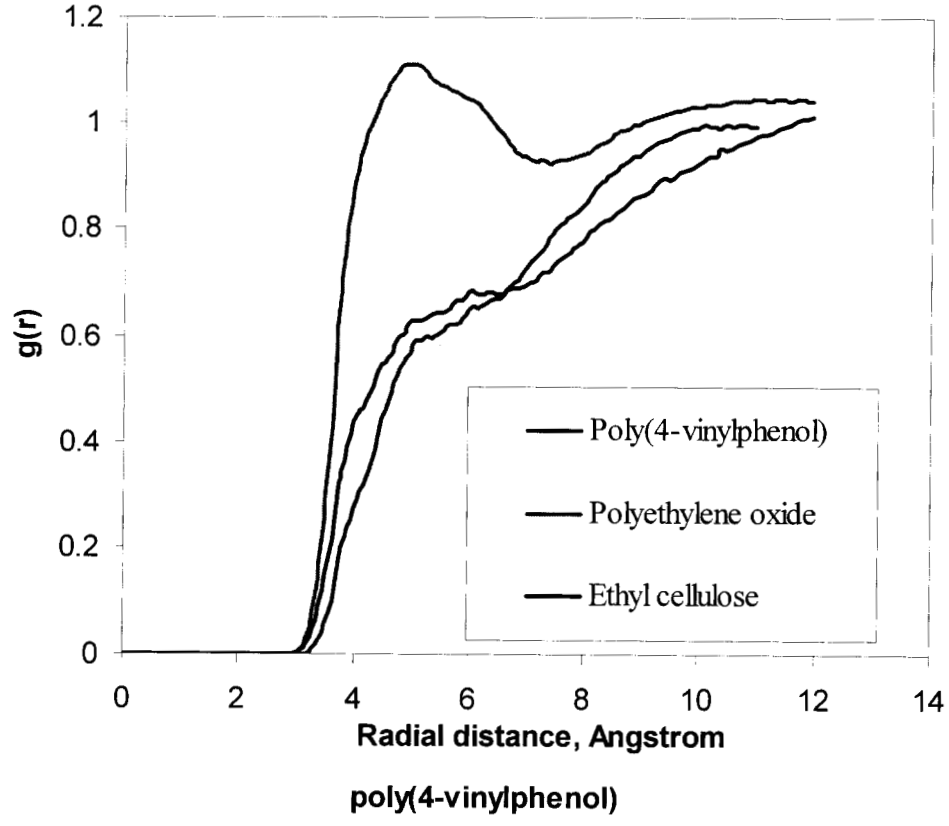


poly(4-vinylphenol)

(b)

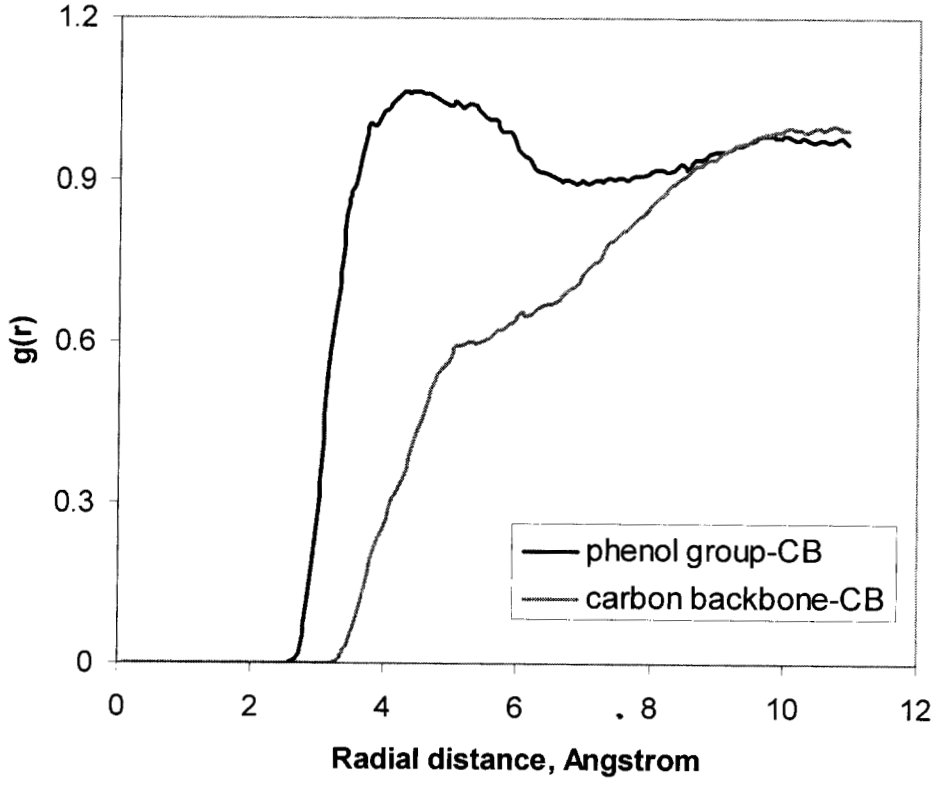

FIGURE 7

(a)

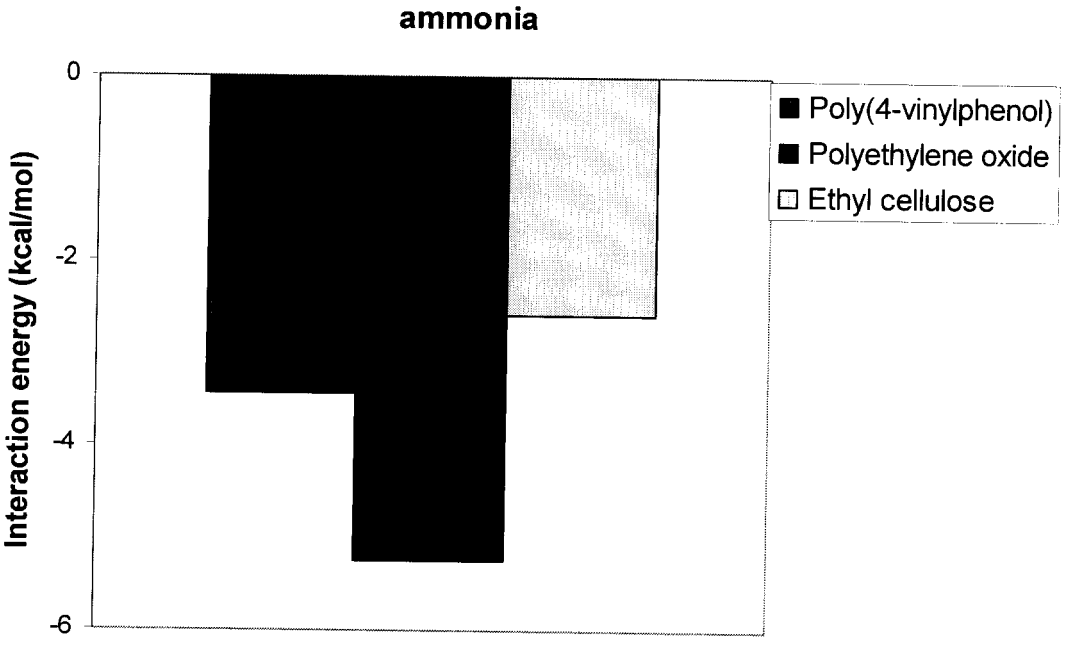
ammonia
0
-2
-4
-6
Interaction energy (kcal/mol)
Poly(4-vinylphenol)
Polyethylene oxide
Ethyl cellulose

(b)

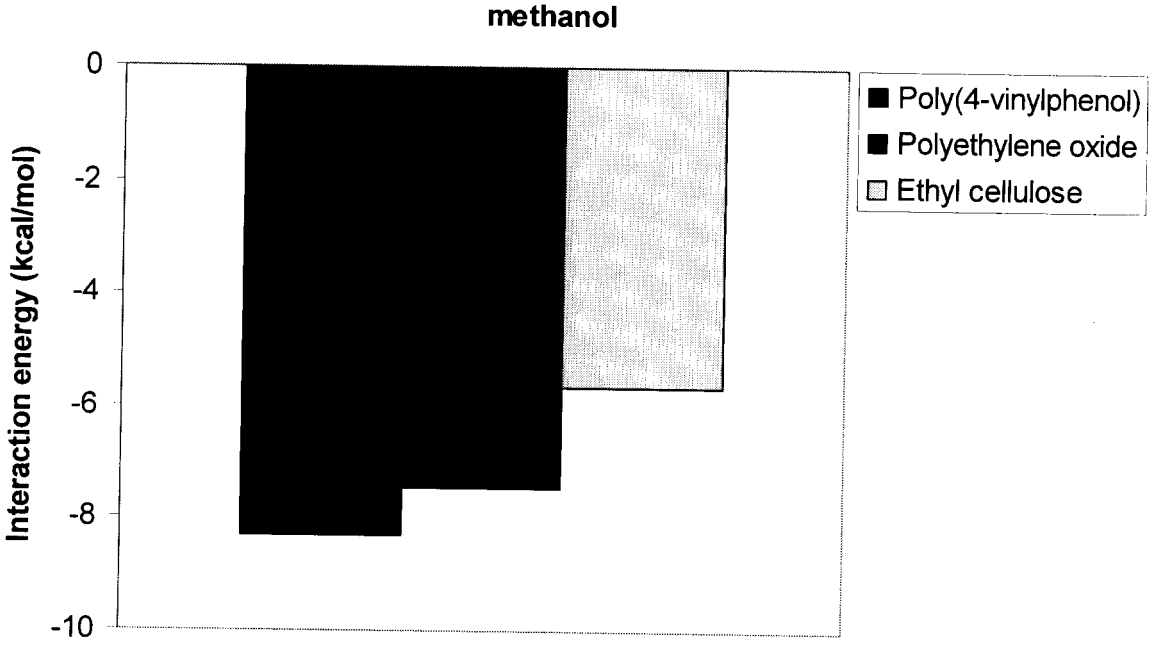
methanol
0
-2
-4
-6
-8
-10
Interaction energy (kcal/mol)
Poly(4-vinylphenol)
Polyethylene oxide
Ethyl cellulose

**FIGURE 7 (Contd.)**

(c)

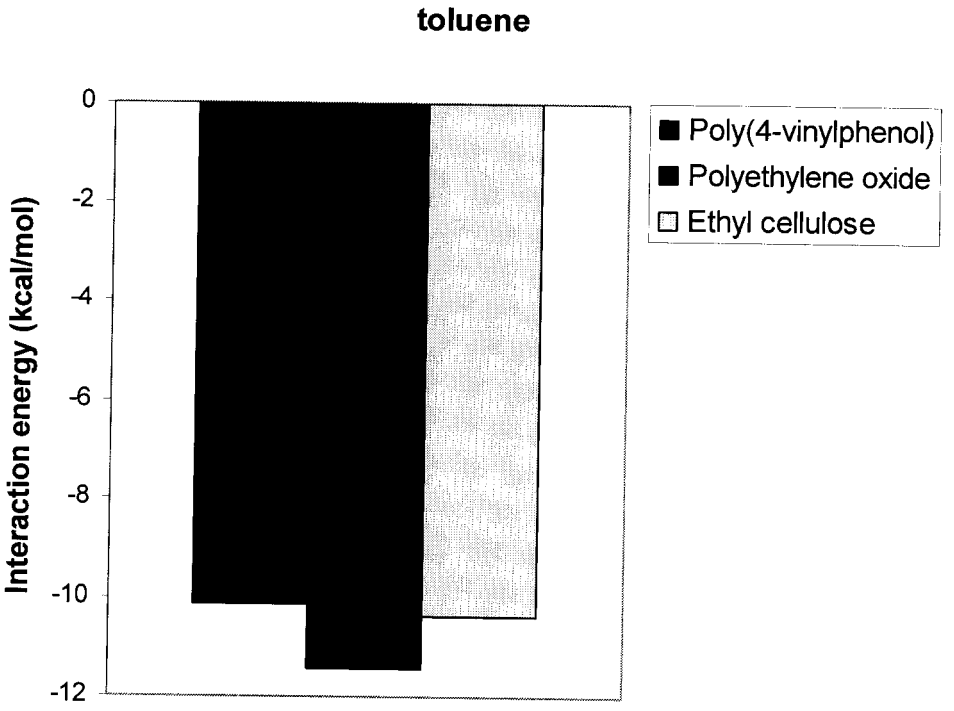


(d)